EuroSun2026

Economic and technical optimization of solar district heating concepts based on local renewable energies and seasonal thermal energy store for rural villages in Germany

Katharina Zimmer[1], Harald Drück[1], Jürgen Lemke[2], Elisa Overbeck[1], Konstantinos Stergiaropoulos[1]

[1]*Institute for Building Energetics, Thermotechnology and Energy Storage (IGTE)*
University of Stuttgart, Germany

[2]*Bürgerenergiegenossenschaft Müsen eG*

katharina.zimmer@igte.uni-stuttgart.de

Summary

To achieve climate neutrality in the heating sector, the transition from decentralized fossil-fuel systems to solar district heating networks is a key component, as this approach enables rapid decarbonization. This investigation uses a simulation-based parameter study to examine the feasibility of a climate-neutral district heat supply, using the example of Müsen in North Rhine-Westphalia, Germany, with around 2,200 inhabitants and a heat demand of approximately 7,000 MWh/a. The analysis examines the influence of Borehole Thermal Energy Storage (BTES) volume and collector area, while evaluating two collector types, various BTES charging strategies, and the integration of power-to-heat (P2H) using excess electricity. Results identify an economically optimal configuration consisting of a BTES volume of 402,000 m^3 (400 boreholes, 80 m depth, 4 m spacing) and a flat-plate collector area of 25,000 m^2. Evacuated tube collectors achieved equivalent system efficiency with a 24 % reduction in required area (19,000 m^2) compared to flat-plate collectors. Furthermore, comparing BTES charging temperatures of 60 °C and 90 °C revealed that higher temperatures reduce heat pump electricity consumption by 7.5 % for flat-plate and 9.6 % for evacuated tube collectors, though this increase significantly raises stagnation hours. Finally, the integration of P2H demonstrates that CO_2 emissions from heat pump operation decrease as the availability of excess electricity increases. However, this reduction is currently largely achieved by displacing solar energy, resulting in a lower solar fraction and increased stagnation compared to a reference system model.

Keywords: solar district heating, seasonal thermal energy store, system simulation, innovative operating strategies, TRNSYS, system simulation

Field of application for the findings: Sustainable and Efficient Districts

Addressed audience: Researchers, engineers, and practitioners in the fields of sustainable district heating concepts, seasonal thermal energy store and system simulations, decision makers of municipalities

1. Introduction

Achieving climate neutrality requires a significant acceleration of the energy transition in the heating sector which is currently not progressing enough to meet the established German decarbonization targets. Most residential buildings in small German towns have decentralized, fossil-fuel-powered heating systems. According to Volk et al. (2025), setting up a solar district heating network results in a substantially faster decarbonization than individual renovations combined with heating system conversions. Over time, this results in significant absolute reductions in CO_2 emissions. Regarding the decarbonization of heat supply, district heating systems enable the economically viable use of seasonal energy stores to maximize the use of local renewable energies, such as solar thermal energy (Raab et al., 2004).
To support heat suppliers in implementing seasonal heat stores and integrating them into district and local heating networks, the "URBAN ARENA" initiative was launched (Projektträger Jülich, 2026b). Furthermore, URBAN ARENA aims to set standards for the installation of seasonal heat store systems. However, with regard to rural areas, there currently exists only one solar district heating network with high solar fraction of about 70 % in Germany (Energieforschung, 2025). It is located in Bracht, a small village with around 900 inhabitants,

20 km northeast of Marburg. Further research is required to achieve widespread expansion of solar district heating networks with high solar fraction. The "MultiHeat" project aims to contribute to this by investigating how a combination of local renewable energies, such as solar radiation and a seasonal thermal energy store, can provide a climate-neutral supply of heat and domestic hot water in rural residential areas. This is done using the village of Müsen in North Rhine-Westphalia with around 2,200 inhabitants and a heat demand of approximately 7,000 MWh/a as a basis.
This contribution investigates the performance of the proposed district heating system including a Borehole Thermal Energy store (BTES) by conducting a systematic simulation-based parameter study for the village of Müsen as an example. The analysis examines the influence of the BTES volume and collector area, compares two collector types, evaluates different BTES charging strategies, and investigates the integration of power-to-heat (P2H) using excess electricity. The economic evaluation has not yet been completed, as reliable cost data from multiple suppliers are still required. The economic assessment will be finalized once sufficient and comparable cost data are available.

2. State of the art

With more than 4,000 installations in Germany, district heating networks are a well-established technology for efficient heat supply, particularly in urban areas. However, approximately two-thirds of the heat supplied by existing district heating networks is generated from fossil fuels, with fossil gas being the primary source. In addition, the majority of heat supply from non-fossil sources comes from biomass and waste. In contrast, heat pumps as well as solar and geothermal energy account for about 2 % of the existing district heating supply. (AGFW, 2025)
Seasonal thermal energy stores enable the integration of significant shares of solar heat into district heating by storing solar energy generated in summer for use during the winter heating season. While solar district heating with seasonal stores has been demonstrated in several large-scale systems (Bauer et al., 2016; Drück et al., 2022; European Commission, 2015), its application in rural areas remains limited. Low heat densities and small network sizes can increase specific investment costs and challenge economic feasibility. In rural areas, local structures, including cooperatives, volunteering and locally available operational support, can help offset these structural disadvantages and improve economic viability of rural district heating systems. Consequently, the economic viability of such rural configurations depends on a precise techno-economic optimization of the seasonal storage and energy source integration

3. Simulation model

Figure 1 shows the schematic illustration of the basic configuration of the investigated solar district heating system of Müsen, including the main components: a collector filed, buffer stores, a BTES and a heat pump (HP).

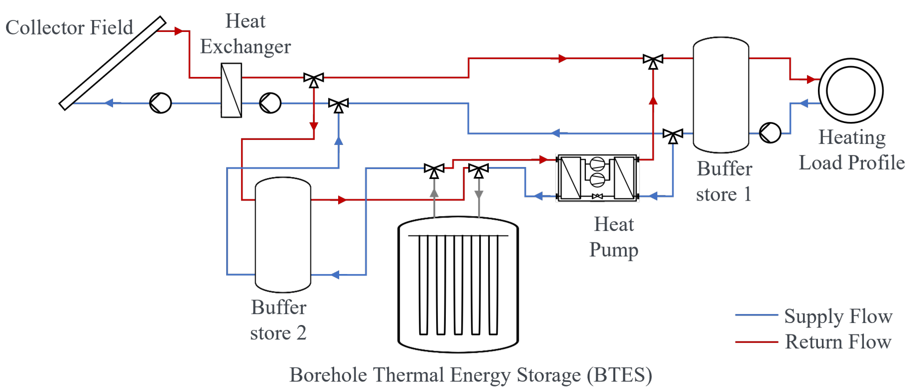

Fig. 1: Schematic illustration of the basic structure of the Müsen solar district heating system

The simulation model of the investigated solar district heating system has been created with the simulation software TRNSYS Version 18. This software is commonly used for detailed dynamic simulation of energy systems, especially in the scientific and research community. To model the overall solar district heating system, sub-models are used for each individual component. The simulations were conducted at 10-minute intervals over a period of six years to allow the seasonal energy store to reach a stationary steady state. For the evaluation of the simulation results, only the data of the final year of the six-year simulations was considered. The most important system's sub-models are presented in the following.

3.1 Sub-models

For modeling solar thermal collectors the TRNSYS "Type 1a" was used. The collector efficiency parameters for the modeled flat-plate collectors and evacuated tube collectors are given in Table 1.

Tab. 1: Collector efficiency parameters

Collector type	Peak efficiency [-]	First-order heat-loss coefficient [W/(m^2·K)]	Second-order heat-loss coefficient [W/(m^2·K^2)]
Flat-plate collector	0.782	2.27	0.018
Evacuated tube collector	0.719	1.45	0.0051

Buffer stores were modeled using TRNSYS "Type 340" by Drück (2007). These stores are directly charged and discharged without using a heat exchanger. The buffer store model considers thermal stratification and heat losses to the environment. In this district heating system, buffer stores are used to allow a continuous operation of the heat pump and the solar collectors. Additionally, they hydraulically separate different parts of the district heating system.

The borehole thermal energy store (BTES) was modeled using TRNSYS "Type 557b" which implements the Duct Ground Heat store Model (DST) developed by Hellström (1989). The thermal resistance for the borehole heat exchangers and the ground's thermal conductivity were identified through a geothermal response test.

The heat pump was modeled using an Equation component. The condenser's power was calculated based on the heat demand of the district heating load profile. The evaporator power and compressor power were calculated using the supply temperatures of the load file and Equation (1).

$$\mathrm{COP} = 0.0000002\,\vartheta_{\mathrm{ev,out}}^{4} - 0.0000631\,\vartheta_{\mathrm{ev,out}}^{3} + 0.0037\,\vartheta_{\mathrm{ev,out}}^{2} - 0.0016\,\vartheta_{\mathrm{ev,out}} + 2.4371 \tag{1}$$

with

$\vartheta_{\mathrm{ev,out}}$: evaporator outlet temperature [°C]

This equation models the Coefficient of Performance (COP) curve for the Carrier heat pump type "61XWH-ZE" as a function of the evaporator outlet temperature $\vartheta_{\mathrm{ev,out}}$ and reaches a plateau at an evaporator outlet temperature of 50 °C.

3.2 Input Data

The weather data was chosen according to the synthetic load profiles by Fraunhofer ISE (2024) that were published with the corresponding weather data for Test Reference Year (TRY) 2010 from "Deutscher Wetterdienst[1]" (DWD) for a weather station in Bad Marienberg, Rhineland-Palatinate. Although the present study focuses on a district heating network in Müsen in North Rhine-Westphalia, the Bad Marienberg weather data are used because they are directly associated with the available load profiles. Since the two locations are approximately 40 km apart as straight-line distance, it was assumed that the weather data provides a reasonable approximation of the weather conditions at the study location. Figure 2 shows the hourly and monthly weather data at the weather station in Bad Marienberg of TRY 2010. The total annual global irradiance is 972 kWh/m^2 and the annual mean ambient temperature is 7.8 °C.

The annual heat demand for the village of Müsen was estimated based on the evaluation of 265 questionnaires that the local citizen energy cooperative had distributed to residents regarding their interest of connecting to the planned solar district heating network, their current heat and domestic hot water consumption as well as

[1] German Meteorological Service

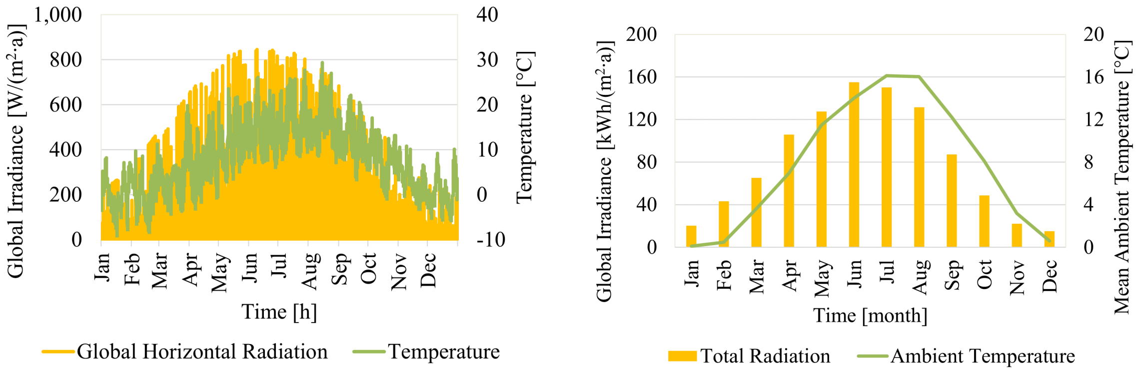

(a) Hourly weather data

(b) Monthly weather data

Fig. 2: Hourly and monthly weather data for TRY 2010 at the weather station Bad Marienberg

their heating type. The resulted heat demand was extrapolated from 265 to 320 consumers of the planned solar district heating network resulting in annual heat demand of 7.2 GWh/a. The heat loss rate of the district heating network of 24 % of the annual heat demand was calculated using simplified TRNSYS simulations of the piping. This resulted in a total heat demand of 8.9 GWh/a.

Heating and domestic hot water load profiles were generated using the synPRO Tool by Fraunhofer ISE https://synpro-lastprofile.de/. The free data set includes four different residential building load profiles: single-family and multi-family houses, each for Passive Houses and for buildings constructed between 1979 and 2001. In addition, load profiles are available for office buildings, schools, and restaurants. These profiles were weighted according to the local building structure and scaled to match the expected annual heat demand of the district heating network. To account for realistic simultaneity effects, temporal shifts were applied to the individual load profiles prior to aggregation. Finally, the resulting total load profile for the village of Müsen was smoothed to reduce high-frequency fluctuations, providing a representative input for a numerically stable subsequent simulation. Figure 3 shows the total heat load profile of the village of Müsen.

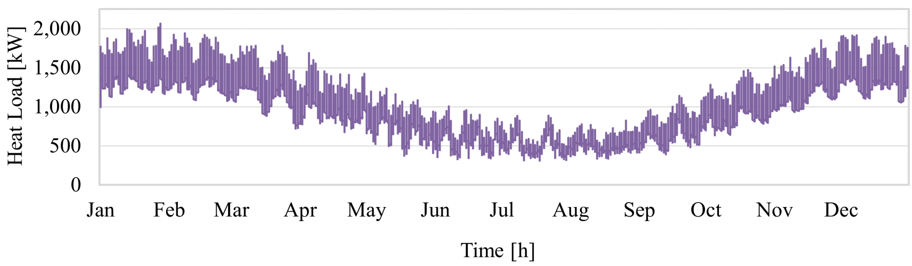

Fig. 3: Total heat load profile of the planned district heating network in the village of Müsen

To meet the hygiene criteria for domestic hot water supply, the supply temperature follows a heating curve with at least 70 °C that increases at ambient temperatures of -5 °C or lower. The spread of the the return and supply temperature was set to 15 K. The resulting grid temperature profile is presented in Figure 4.

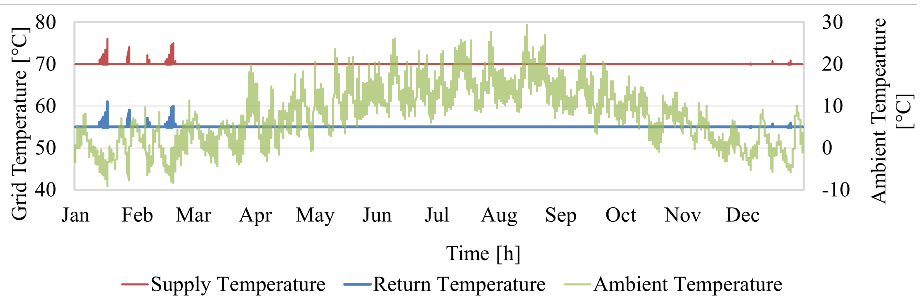

Fig. 4: Grid temperature profile and ambient temperature of the planned district heating network in the village of Müsen

In the village of Müsen, the available area for solar collectors, a seasonal energy store and other components of the district heat supply is restricted to about 4 ha. Therefore, the maximum possible collector area is about 2 ha, due to minimum spacing between collectors to prevent shading.

3.3 Control strategy

The goal of the control strategy is to minimize the CO_2 emissions from electricity consumption while maintaining district heating prices as low as possible. The control strategy for distributing the solar energy follows the following priorities:

1. The grid's buffer store is supplied with solar energy, when the collector temperature is sufficient to meet the grid's heat load.
2. The BTES buffer store is supplied with solar energy, when the collector temperature exceeds the lower temperature of the BTES buffer store. Meanwhile the collector temperature is insufficient to meet the grid's heat load or the grid's buffer store top temperature exceeds 95 °C.
3. The grid's buffer store is supplied with solar energy, when the collector temperature exceeds the lower temperature of the grid's buffer store while the BTES buffer store top temperature exceeds 60 °C.

The BTES has its own buffer store to charge the BTES with constant heat load using the solar energy collected throughout the day for a period of approximately 24 hours. This way the borehole pipes do not need to be designed to handle the maximum solar heat load. Since the supply temperature for the plastic borehole pipes is limited to a maximum of 60 °C to ensure durability, the BTES buffer store has an upper limit of 60 °C as well. The heat pump is activated when the temperature level of the available solar energy is insufficient to meet the heat demand and the BTES outlet temperature exceeds 15 °C. The depth of the BTES boreholes is equivalent to its radius to minimize the thermal losses by minimizing the relation of surface and volume.

4. Simulation results

The relevant evaluation criteria for the performance of the solar district heating systems investigated are the specific solar collector yield, the annual solar fraction, the heat pump's electricity consumption and the stagnation hours of the solar collector field.
The annual solar fraction is calculated as shown in Equation 2 and 3, taking into account thermal losses of the system's buffer stores.

$$f_{\text{sol}} = \frac{Q_{\text{sol}}}{Q_{\text{buf,grid}}} = \frac{Q_{\text{BTES,HP}} + Q_{\text{sol,buf}} - Q_{\text{buf,loss,sol+HP}}}{Q_{\text{buf,grid}}} \tag{2}$$

and

$$Q_{\text{buf,loss,sol+HP}} = \frac{Q_{\text{BTES,HP}} + Q_{\text{sol,buf}}}{Q_{\text{BTES,HP}} + Q_{\text{sol,buf}} + W_{\text{HP,el}}} \cdot Q_{\text{buf,loss}} \tag{3}$$

with

f_{sol}:	annual solar fraction [%]
Q_{sol}:	heat generation solar collector field [MWh/a]
$Q_{\text{buf,grid}}$:	heat consumption grid [MWh/a]
$Q_{\text{BTES,HP}}$:	heat generation heat pump [MWh/a]
$Q_{\text{sol,buf}}$:	heat generation solar collector field directly supplied to the grid buffer [MWh/a]
$Q_{\text{buf,loss,sol+HP}}$:	share of buffer heat losses supplied by solar energy and the heat pump [MWh/a]
$W_{\text{HP,el}}$:	electricity consumption heat pump [MWh/a]

The specific solar collector yield is defined as the annual heat output of the collector per square meter collector area. The heat pump's electricity consumption is determined by its operation time and efficiency which is indicated by the SPF. The SPF is defined as the ratio of the total useful thermal energy supplied by the heat pump to the total electrical energy consumed over the considered period. Stagnation occurs when the heat generated by the solar collector field cannot be utilized. As a result, the collector mass flow rate is reduced to zero, causing the collector temperature to rise until it reaches a stagnation temperature. Based on this definition, in the simulation, stagnation is reached when the collector mass flow is zero, the grid buffer is charged, the solar radiation on the collector surface is greater than 200 W/m^2 and the collector temperature is above 120 °C.

4.1 Parameter study

A parameter study varying the collector area, the number of boreholes and the borehole spacing was conducted, resulting in 100 combinations. The buffer store volume for the grid and BTES was set to 1,500 m^3. Numerous configurations with a relatively small number of boreholes or wide borehole spacing as well as a small collector area were unable to meet the heat demand and were therefore not considered for further evaluation.
Figure 5 shows a strong correlation between the electricity consumption of the HP and the specific solar collector yield for variations of the collector area and the number of boreholes as well as borehole spacing to determine the optimal BTES configuration and collector area.
The results reveal distinct clustering based on the collector area, where smaller areas correlate with higher specific yields as well as higher electricity consumption of the heat pump.

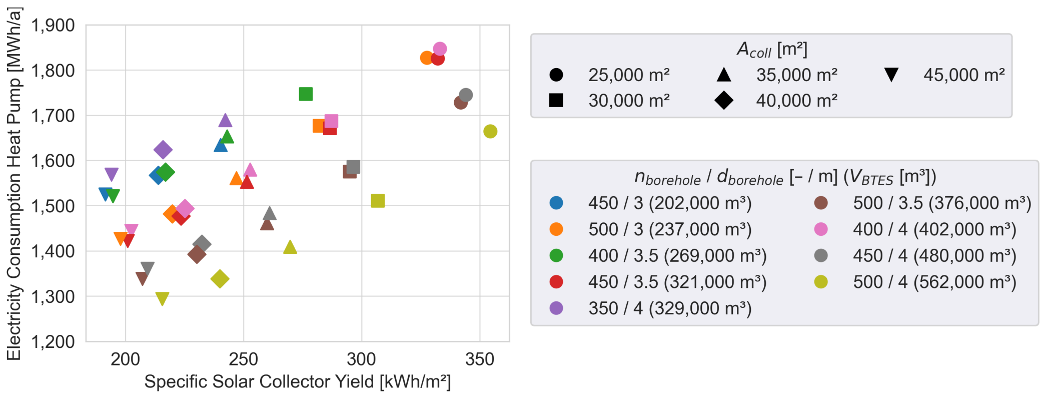

Fig. 5: Electricity consumption of the heat pump (HP) versus specific solar collector yield for flat-plate collectors with variation of collector area and BTES volume with a constant buffer store volume of 1,500 m^2

The specific solar collector yield increases with decreasing collector area because lower total heat production results in less frequent periods of excess heat that can not be stored and consequently lower operating temperatures and thermal losses. At the same time, the lower total heat production of the smaller collector field increases heat pump operation and consequently results in higher electricity consumption. The BTES volume does not correlate with the heat pump's electricity consumption or specific solar collector yield. For several BTES configurations, the electricity consumption and the specific solar collector yield are almost similar, such as 400 boreholes spaced 4 m apart, 450 boreholes spaced 3.5 m apart and 500 boreholes spaced 3 m apart, due to similar total boreholes lengths. The total borehole length is the product of the number of boreholes and the borehole depth which varies for every configuration. The resulting optimal borehole depths regarding the surface-volume-ratio and total borehole lengths are presented in Table 2. This indicates, that the heat pump's electricity consumption and specific solar collector yield correlate with the total borehole length.

Tab. 2: Comparison of borehole configurations with similar results regarding electricity consumption and specific solar collector yield

A_{coll} [m^2]	Number of Boreholes [-]	Borehole Spacing [m]	Borehole Depth [m]	Total Borehole Length [m]
25,000	400	4	80	32,000
25,000	450	3.5	74	33,300
25,000	500	3	67	33,500

To determine the economically optimal BTES configuration within the investigated ranges and parameters, the annuity for the BTES and the collector field were calculated in accordance with VDI 2067 over a period of 25 years at an interest rate of 5 % and an inflation rate of 2 %. For the heat pump and solar collector pump operation an electricity price of of 180 €/MWh was assumed (BDEW, 2026). The specific costs for flat plate collectors was assumed to be 400 €/m^2. Based on a quote from a BTES construction company from the year 2025, the investment cost for the BTES were calculated, resulting in specific costs ranging from 25 and 100 €/m^3, depending on the total borehole length. Figure 6 shows the annuity for the BTES and the collector field for each configuration of the parameter study versus the collector area.

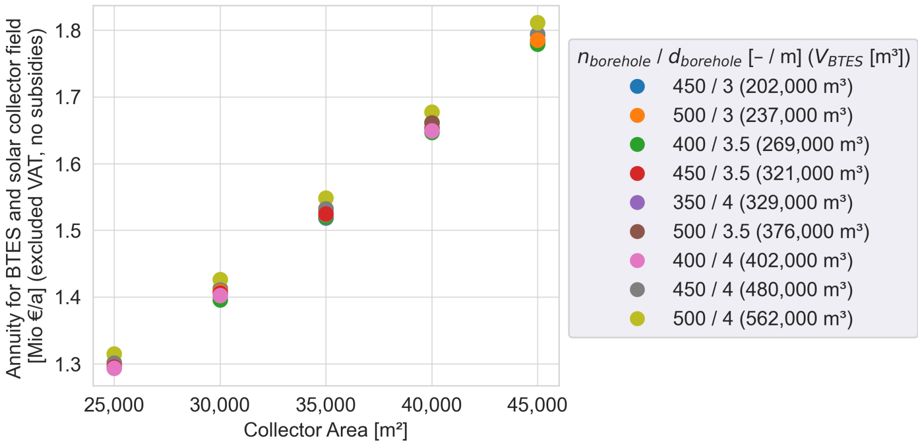

Fig. 6: Annuity for the BTES and solar collector field over the collector area with variation of BTES volume with a constant buffer store volume of 1,500 m^2

The results show a clear clustering of the annuity based on the collector area, with smaller collector areas correlating with lower investment costs. In contrast, the annuity only varies slightly between different BTES configurations, indicating that collector costs have a greater effect on the annuity than BTES costs. From an economic perspective the collector area should be kept as small as possible. As the available area in Müsen is limited, a small collector area is preferable in any case.

Based on the brief economic evaluation, the economically optimal option within the selected parameters and their investigated ranges is a flat-plate collector area of 25,000 m^2 and a BTES configuration with 400 borehole spaced 4 m apart resulting in a BTES volume of about 402,000 ^{3}. For following simulations this configuration is used as reference system model.

4.2 Collector types

Suitable collector types for district heating supply are usually flat-plate and evacuated tube collectors. Because evacuated tube collectors operate more efficiently and reach higher temperatures, they require a smaller collector area than flat-plate collectors to supply an equivalent quantity of heat.

To compare the two collector types under equivalent performance conditions, the collector area of the evacuated tube system was varied until the heat pump's electricity consumption and annual solar fraction (f_{sol}) matched that of the flat-plate reference system. The simulation results for the flat-plate collector (FPC) and evacuated tube collector (ETC) systems are presented in Table 3. compares the simulation results for the flat-plate collector (FPC) and evacuated tube collector (ETC) systems.

Tab. 3: Performance comparison of the district heating model with flat-plate collectors (FPC) and evacuated tube collectors (ETC) at collector areas resulting in similar system efficiency

Collector Type	A_{coll} [m^2]	Electricity Consumption HP [MWh/a]	f_{sol} [-]	q_{coll} [kWh/m^2]	Stagnation hours [h/a]
FPC	25,000	1,847	0.79	333	14
ETC	19,000	1,822	0.79	439	26

Due to higher efficiency of the ETC, a smaller collector area of 19,000 m^2 was sufficient to achieve the a similar heat pump's electricity consumption and annual solar fraction compared to the FPC with a collector

area of 25,000 m^2, corresponding to a reduction in required collector area of approximately 24 %. As a result, the specific solar collector yield increased for the ETC system, since a similar amount of heat was supplied from a smaller area. From a space-use perspective, this makes the ETC advantageous, which is relevant given the limited available area in Müsen. From an economic perspective, however, this area reduction does not compensate for the higher specific investment cost of the ETC. With specific collector cost of 600 €/m^2 for evacuated tube collectors, the total collector investment cost of for 19,000 m^2 EPC system is about 11 % higher than that for 25,000 m^2 of the FPC system. Since the available area in Müsen is limited, a smaller collector area is preferable, despite the increase in investment cost.
The number of stagnation hours also increased for the ETC system compared to the FPC system. Flat-plate collectors have relatively high thermal losses to the ambient environment, which passively limits the maximum collector temperature and reduce the risk of stagnation. Evacuated tube collectors suppress these losses much more effectively due to their vacuum insulation. While advantageous for heat generation, this also means excess heat cannot be dissipated as easily during periods of low demand or high solar radiance, causing the ETC system to reach stagnation more quickly and remain in stagnation longer.

4.3 Influence of inlet temperature of the BTES

Usually the BTES boreholes are equipped with polymeric pipes through which the heat transfer medium is circulated. Standard polymeric pipes allow for constant operating temperatures of up to 60 °C with a design life of up to 50 years. However, in summer, solar collectors supply heat at significantly higher temperatures. With higher BTES inlet temperatures, it is expected that the specific solar collector yield and the annual solar fraction increase. The heat pump's electricity consumption is expected to decrease due to higher BTES temperatures that allow for a higher SPF. To realize this idea, high temperature proof pipes, made from metals or polymers, need to be used in the core of the BTES that is supplied with high inlet temperatures. While the latter are expected to be more expensive, they could still be economically viable if the dimensions of the solar collector field, the BTES and the heat pump as well as their operating costs can be reduced.
The system configurations resulting from Sections 4.1 and 4.2 were operated with a maximum BTES inlet temperature of 60 °C and 90 °C for flat-plate and evacuated tube collectors. Figure 7 shows the heat pump's electricity consumption versus the specific solar collector yield as well as the the annual solar fraction for varied BTES inlet temperatures for flat-plate (FPC) and evacuated tube collectors (ETC).

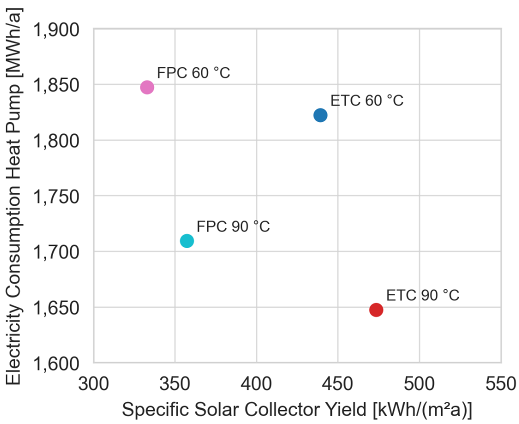

(a) Electricity consumption heat pump versus specific solar collector yield

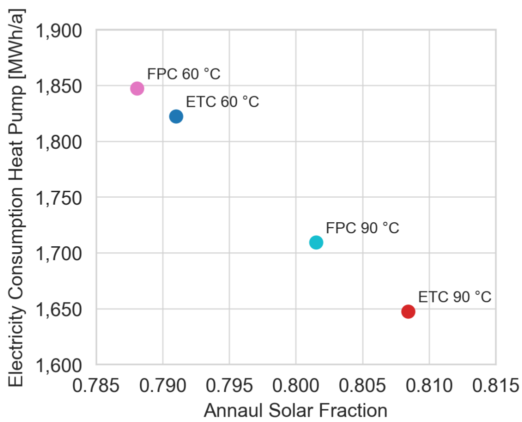

(b) Electricity consumption heat pump versus annual solar fraction

Fig. 7: Simulation results for maximum BTES inlet temperatures of 60 °C and 90 °C for flat-plate (FPC) and evacuated tube (ETC) collectors

With higher BTES inlet temperatures the annual solar fraction increased slightly, by about 2 % for both collector types, less than expected. The specific solar collector yield increased as well, by about 7.5 %. At the same time, stagnation hours rose by 18 % for flat-plate collectors (14 to 16.5 h) and by 27 % for evacuated tube collectors (26 to 33.5 h), since the generallly higher collector operating temperature reduced the buffer before the collectors reached stagnation conditions. The heat pump's electricity consumption decreased notably, by about 7.5 % for flat-plate collectors and 9.6 % for evacuated tube collectors, showing that the main advantage of high BTES inlet temperatures is the reduced heat pump's electricity consumption which reduces the operational costs. Another advantage could be the possible smaller dimensions of the BTES, collector area, and buffer stores, which needs to be investigated. However, a final recommendation would require a cost-benefit analysis of the increased investment costs of high-temperature borehole pipes against the reduction of operational costs and probably smaller dimensions of the main components. Due to the limited number of manufacturers offering high-temperature borehole pipes and the lack of established research on this design approach, no reliable cost data are currently available.

5. Innovative control strategies

High shares of renewable power installations produce volatile electricity generation, which causes redispatch costs in the current electricity grid. For operators of district heating systems, using this excess renewable electricity for power-to-heat (P2H) is a cost-effective and sustainable option. Therefore, the model will be extended by P2H from local excess renewable energies.

5.1 Data collection

Historical high-resolution data on excess renewable electricity is not directly available, as excess electricity generation is curtailed due to grid constraints. Negative and very low historical wholesale electricity prices can indicate periods of excess renewable electricity generation. Data on wholesale electricity prices was retrieved from (Bundesnetzagentur, 2025). From this data, no conclusions can be drawn regarding the available amount of excess electricity generation. In addition, the data is not available in regional resolution. Using local weather data, the profile of electricity generation from wind and photovoltaic can be estimated. The installed capacity can be retrieved from several websites, depending on the region. To estimate the excess electricity generation, the local renewable energy generation must be balanced against the local electricity consumption. Since it is politically planned to continuously increase the share of renewable electricity generation, the potential of excess electricity for P2H will increase and should therefore be evaluated based on future data.

Future data on excess electricity generation was derived from SimBench datasets (Meinecke et al., 2020). SimBench pairs geographically and statistically derived German network models with consistent, full-year, quarter-hourly profiles for load, storage, and renewable generation. These profiles draw on sources like OpenStreetMap, official statistics, demand data, and DWD weather data, processed via an agent-based simulation tool. SimBench offers multiple datasets across different voltage levels and demographic contexts, each with three scenarios (2016, 2024, and 2034) representing a validated baseline and two future projections with rising renewable shares, load growth, and grid expansion, enabling analysis of the grid's evolution through the energy transition.
From a SimBench dataset for a medium-voltage level in a rural area, 15-minute-resolution profiles of renewable electricity generation, electricity demand, and storage were extracted and time-aligned to calculate the local renewable electricity surplus. To convert the profile according to the scope of Müsen, with about 2,200 inhabitants, a scaling factor of 0.165 was estimated based on an average annual electricity demand of about 1,600 kWh per person (Statistisches Bundesamt, 2024) and a share of electricity demand of households of 60 %. The 2016 baseline scenario was used as the reference for excess electricity, as it most closely reflects the existing electricity grid. A second profile, representing excess electricity in 2030, was interpolated from the 2024 and 2034 forecasts. Figure 8 shows the profile of estimated local excess electricity from renewable energies based on the SimBench data set in 2016 and 2030.

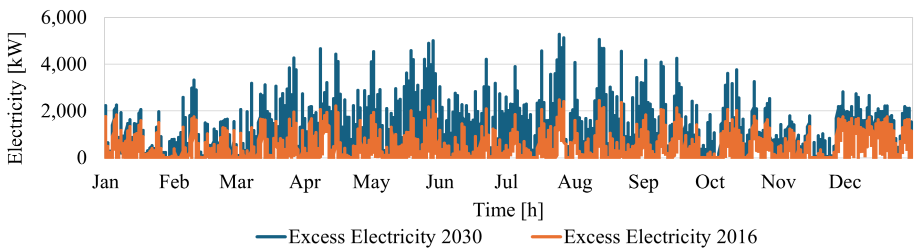

Fig. 8: Profile of estimated local excess electricity from renewable energies 20for Müsen based on SimBench data set for 2016 and 2030

5.2 Extended system simulation model

The reference system model was extended by an electric boiler with an efficiency of 0.99 that runs exclusively on excess electricity from local renewable sources and provides heat at 95 °C for the grid's buffer store with a maximum electric power of 500 kW. Since there is an additional heat source in the model, the collector area of the flat-plate collectors was reduced to 20,000 m^2 compared to the reference system model identified in Section 4. The simulations were conducted for the reference BTES configuration The control strategy was extended using the data presented in Section 5.1. If the electricity production from renewable energies is higher than the electricity load, the electric boiler operates between 50 and 500 kW, depending on the available excess electricity.

5.3 Simulation results

In addition to the assessment criteria used in the sections above, the CO_2 emissions of the energy required for system operation are compared, which are mainly driven by the heat pump's electricity consumption. According to BAFA (2025), a CO_2 factor of 0.107 t CO_2/MWh was applied. Figure 9 illustrates the difference of assessment criteria between the P2H system models and the reference system model.

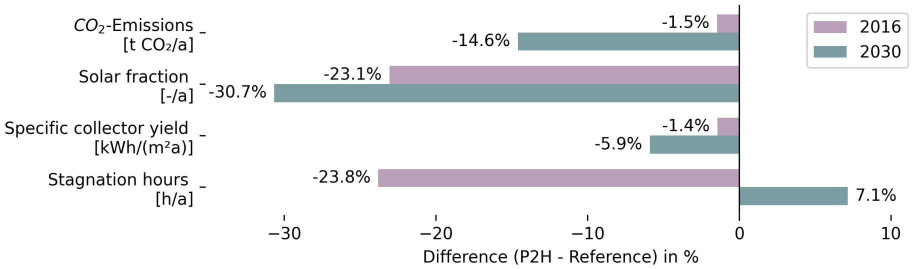

Fig. 9: Difference of selected criteria from simulation studies of P2H system models and reference system model

Compared to the reference system, CO_2 emissions decreased slightly in the 2016 scenario and by about 15 % in the 2030 scenario. In both scenarios the annual solar fraction dropped drastically, which suggests that excess electricity partly replaces solar energy in covering the heat demand. To test whether the reduced collector area explains this, simulations were repeated using the reference collector area of 25,000 m^2, which did not alter the results significantly. This suggests the drop in solar fraction is mainly caused by the displacement effect. A different control strategy could probably reduce this effect. The results may also point to a frequent temporal overlap between the availability of excess renewable electricity and solar radiance. The specific solar collector yield decreased only slightly by about 6 % in the 2030 scenario. This can be explained by the fact that the solar collector yield depends primarily on solar radiance and the operating conditions of the collector loop, both of which are largely unaffected by the P2H implementation. Stagnation hours decreased by about 24 % in the 2016 scenario and increased by about 7 % in the 2030 scenario. In 2030, more excess electricity is available, so the electric boiler often covers the heat load before solar heat can be used, causing the collector to reach stagnation. In 2016, less excess electricity is available, so this conflict happens less often. In addition, the smaller collector area compared to the reference scenario leads to fewer stagnation hours in both cases.

Figure 10 shows the shares of the heat supply to the grid for the P2H system models and the reference system model.

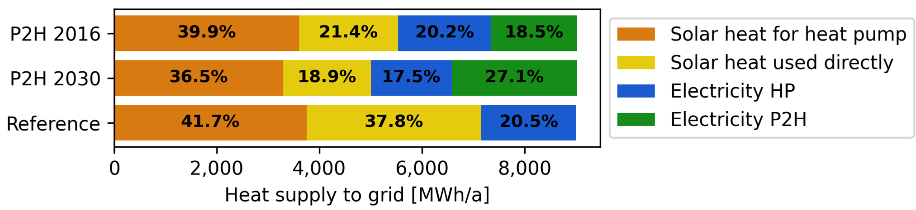

Fig. 10: Heat supply to the grid for the models with P2H and the reference system model

In the 2016 scenario, about 19% of the total heat demand is covered by excess electricity, and in the 2030 scenario this share rises to about 27%. This increase reflects the greater availability of excess renewable electricity assumed for 2030. The results show that the heat supplied by the heat pump decreased only slightly compared to the reference system, while the direct use of solar energy dropped by almost half in both scenarios. This indicates that the excess electricity mainly displaces direct solar heat rather than heat pump operation. It is notable that the drop in direct solar use is of similar relative size in both scenarios, even though the share of excess electricity is considerably higher in 2030 than in 2016. This suggests that the displacement of solar heat by excess electricity reaches a kind of saturation, since only a limited number of hours exist in which solar heat and excess electricity are both available at the same time. Once most of these overlapping hours are already covered, additional supply in 2030 mainly reduces the heat pump's share instead. This is consistent with the larger difference in CO_2 emissions between the two scenarios reported above, as electricity increasingly substitutes for heat pump operation rather than solar heat once the overlap potential with solar radiation is exhausted. Since the system simulations performed for the P2H concept relied on future-predicted data whose actual values and operation conditions cannot yet be verified, the results are subject to significant uncertainty.

6. Conclusion

This contribution investigated the performance of a district heating system through a parameter study, a comparison of collector types, an alternative BTES charging approach, and the integration of power-to-heat (P2H) using excess electricity, with the town of Müsen in North Rhine-Westphalia serving as a case study.
The parameter study identified a BTES volume of 402,000 m^3, corresponding to 400 boreholes with a spacing of 4 m and a depth of 80 m and a collector area of 25,000 m^2, as the economically optimal configuration within the investigated range. For the resulting BTES volume with collector areas between 25,000 and 45,000 m^2, the heat pump's electricity demand ranged from 1,300 to 1,850 MWh/a and the solar fraction from 0.79 to 0.85.
The comparison of flat-plate and evacuated tube collectors showed that with the latter a smaller collector area of 19,000 m^2 was sufficient to achieve a similar system efficiency compared to the FPC with a collector area of 25,000 m^2, corresponding to a reduction in required collector area of approximately 24 % and an increase of 11 % in investment costs for the collector field. Since the available area in Müsen is limited, a smaller collector area was preferable, despite the increase in investment cost.
The comparison of BTES charging temperatures of 60 °C and 90 °C showed that the main advantage is the reduced heat pump's electricity consumption, by about 7.5 % for flat-plate collectors and 9.6 % for evacuated tube collectors. At the same time, stagnation hours rose significantly for both collector types. A final recommendation would require a cost-benefit analysis. However, due to the limited number of manufacturers offering high-temperature borehole pipes and the lack of established research on this design approach, no reliable cost data are currently available. Future research should also investigate possible smaller dimensions of the BTES, collector area, and buffer stores.
Implementing P2H with estimated excess electricity showed that P2H can reduce CO_2 emissions from heat pump operation, and this effect becomes larger as more excess electricity is available, from a small reduction in 2016 to about 15 % in 2030. However, this reduction is currently largely achieved by displacing solar energy, resulting in a lower solar fraction and increased stagnation compared to a reference system model. Therefore, fully exploiting the emission reduction potential of P2H would likely require a control strategy that uses excess electricity preferably when it does not replace solar heat that is already available. Since the evaluation of the potential of P2H from excess electricity is subject to significant uncertainty, as it is based on future-predicted data and the actual future operating conditions cannot be known today, the observed differences should be interpreted with caution.
Future research should focus on designing and testing a BTES configuration with high-temperature-resistant pipes at its center as well as an improved P2H control strategy that avoids displacing solar heat that is already available.

7. Acknowledgments

The work presented in this contribution is part of the MultiHeat project, funded by the German Federal Ministry for Economic Affairs and Energy (BMWE) as a microproject under funding code 03ENM6005 by the project management agency Jülich (PTJ) on the basis of a resolution by the German Bundestag. The authors gratefully acknowledge this support and carry the full responsibility for the content of this publication.

References

AGFW. AGFW Hauptbericht 2024, December 2025. URL https://www.agfw.de/zahlen-und-statistiken/agfw-hauptbericht/. Accessed: 2026-08-05.

BAFA. Informationsblatt co_2-faktoren, 2025. URL https://www.bafa.de/SharedDocs/Downloads/DE/Energie/eew_infoblatt_co2_faktoren_2025.html.

D. Bauer, H. Drück, S. Lang, R. Marx, and T. Plaz. Weiterentwicklung innovativer Technologien zur solaren Nahwärme und saisonalen Wärmespeicherung : Akronym "WinterSun" : Forschungsberichnt zum BMWi-Vorhaben : Laufzeit des Vorhabens: 01.01.2013 bis 30.09.2015, 2016. URL https://www.tib.eu/suchen/id/TIBKAT:870788035/.

BDEW. BDEW-Strompreisanalyse, 2026. URL https://www.bdew.de/service/daten-und-grafiken/bdew-strompreisanalyse/.

Bundesnetzagentur. SMARD Marktdaten Deutschland. SMARD.de, 2025. URL https://www.smard.de/home/downloadcenter/download-marktdaten/?downloadAttributes=%7B%22superCategoryId%22:3,%22subcategoryId%22:8,%22regionId%22:%22DE%22,%22resolution%22:%22hour%22,%22fileType%22:%22XLS%22,%22from%22:1735686000000,%22to%22:1767221999999%7D. Hourly market data for Germany; downloaded from the SMARD data download centre. Licensed under CC BY 4.0.

H. Drück, N. Bonk, W. Juschka, J. Ullmann, S. Lang, M. Gensbaur, D. Bestenlehner, J. Hübner, E. Reu, and S. Abel. Erweiterung und Optimierung der solaren Nahwärmeversorgung Hirtenwiesen II in Crailsheim sowie Begleitforschung zu solarer Nahwärme und saisonaler Wärmespeicherung; Akronym: "CROW" : Abschlussbericht : Laufzeit des Vorhabens: 01.10.2016 bis 31.12.2021, 2022. URL https://www.tib.eu/suchen/id/TIBKAT:1858912067.

H. Drück. *Mathematische Modellierung und experimentelle Prüfung von Warmwasserspeichern für Solaranlagen*. Berichte aus der Energietechnik. Shaker Verlag, Aachen, Mai 2007. ISBN 9783832262150.

Energieforschung. 100 Prozent regenerativ: Solarwärme liefert Großteil der Wärme für hessisches Dorf, 2025. URL https://www.energieforschung.de/de/aktuelles/news/2025/100-prozent-regenerativ-solarwaerme-liefert-grossteil-der-waerme-fuer-hessisches-dorf. Accessed: 2026-08-05.

European Commission. EINSTEIN: Effective Integration of Seasonal Thermal Energy Storage Systems in Existing Buildings. EU Seventh Framework Programme, Grant Agreement No. 284932, 2015. URL https://cordis.europa.eu/project/id/284932. CORDIS project record.

Fraunhofer ISE. synPRO Tool, 2024. URL https://synpro-lastprofile.de/.

G. Hellström. Duct Ground Heat Storage. *Manual for Computer Code*, 1989.

S. Meinecke, D. Sarajlić, S. R. Drauz, A. Klettke, L. Lauven, C. Rehtanz, A. Moser, and M. Braun. SimBench—A Benchmark Dataset of Electric Power Systems to Compare Innovative Solutions Based on Power Flow Analysis. *Energies*, 13(12):3290, 2020. ISSN 1996-1073. doi: 10.3390/en13123290. URL http://dx.doi.org/10.3390/en13123290.

Projektträger Jülich. URBAN ARENA setzt Grundlagen für saisonale Wärmespeicher, 2026a. URL https://www.energieforschung.de/de/aktuelles/projekteinblicke/urban-arena-start-mikroprojekte-saisonale-waermespeicher. Aktualisiert am 22.06.2026.

Projektträger Jülich. URBAN ARENA Seasonal Heat Storage, 2026b. URL https://www.urbanarenas.org/. Accessed: 2026-08-21.

S. Raab, T. Schmidt, M. Benner, W. Heidemann, and H. Müller-Steinhagen. Saisonale Wärmespeicher – aktuelle Speichertechnologien und Entwicklungen bei Heißwasser-Wärmespeichern. In *OTTI Fachseminar Oberflächennahe Geothermie*, Garching, Germany, February 2004. URL https://www.igte.uni-stuttgart.de/veroeffentlichungen/publikationen/publikationen_04-03.pdf.

Statistisches Bundesamt. Stromerzeugung 2023: 56 % aus erneuerbaren Energieträgern. Pressemitteilung Nr. 087, March 2024. URL https://www.destatis.de/DE/Presse/Pressemitteilungen/2024/03/PD24_087_43312.html. Accessed: 2026-08-11.

P. Volk, C. Schmelzer, O. Kusyy, J. Orozaliev, U. Jordan, and K. Vajen. Erneuerbare Wärmenetzsysteme im ländlichen Raum. In *Proceedings of the 8. RETCon – Regenerative Energietechnik Konferenz*, Nordhausen, 2025.